p-Nitrobenzoate production from glucose by utilizing p-aminobenzoate N-oxygenase: AurF

Mori, Ayana ; Hirata, Yuuki ; Kishida, Mayumi ; Mori, Yutaro ; Kondo, Akihiko ; Noda, Shuhei ; Tanaka, Tsutomu

(Citation)
Enzyme and Microbial Technology,171:110321

(Issue Date)
2023-12

(Resource Type)
journal article

(Version)
Accepted Manuscript

(URL)
https://hdl.handle.net/20.500.14094/0100486184

p-Nitrobenzoate production from glucose by utilizing *p*-aminobenzoate *N*-oxygenase: AurF

Ayana Mori[a], Yuuki Hirata[a], Mayumi Kishida[a], Yutaro Mori[b], Akihiko Kondo[b,c], Shuhei Noda[b], and Tsutomu Tanaka[a*]

[a]Department of Chemical Science and Engineering, Graduate School of Engineering, Kobe University, 1-1 Rokkodai-cho, Nada-ku, Kobe, Hyogo 657-8501, Japan

[b]Center for Sustainable Resource Science, RIKEN, 1-7-22 Suehiro-cho, Tsurumi-ku, Yokohama, Kanagawa 230-0045, Japan

[c]Graduate School of Science, Technology and Innovation, Kobe University, 1-1 Rokkodai-cho, Nada-ku, Kobe, Hyogo 657-8501, Japan

*Corresponding Author: tanaka@kitty.kobe-u.ac.jp

Abbreviations:

PNBA, *p*-nitrobenzoate; PABA, *p*-aminobenzoate

Abstract

Nitroaromatic compounds are widely used in industry, but their production is associated with issues such as the hazardousness of the process and low regioselectivity. Here, we successfully demonstrated the production of *p*-nitrobenzoate (PNBA) from glucose by constructing *p*-aminobenzoate *N*-oxygenase AurF-expressing *E. coli*. We generated this strain, which we named PN-1 by disrupting four genes involved in PNBA degradation: *nfsA*, *nfsB*, *nemA*, and *azoR*. We then expressed AurF from *Streptomyces thioluteus* in this strain, which resulted in the production of 945 mg/L PNBA in the presence of 1 g/L *p*-aminobenzoate. Direct production of PNBA from glucose was achieved by co-expressing the *pabA*, *pabB*, and *pabC*, as well as *aurF*, resulting in the production of 393 mg/L PNBA from 20 g/L glucose. To improve the PNBA titer, we disrupted genes involved in competing pathways: *pheA*, *tyrA*, *trpE*, *pykA*, and *pykF*. The resultant strain PN-4Ap produced 975 mg/L PNBA after 72 h of cultivation. These results highlight the potential of using microorganisms to produce other nitroaromatic compounds.

Keywords:

Nitroaromatic compound; AurF; *E. coli*; *N*-oxygenase; Microbial production

1. Introduction

Most of the chemical products that surround us are manufactured from fossil fuels, but there is a need to shift away from such production in order to achieve a sustainable society. One alternative approach is to use microbial production [1-3]. In this approach, renewable biomass is used as a raw material and engineered microbes are employed to produce the desired chemical compounds. To date, microbial production has been

49 employed to synthesize a wide variety of chemical compounds, such as alcohols [4-6],
50 carboxylates [7-10], organic acids [11-13], and amino compounds [14-19], with the
51 number of such compounds produced by microbes increasing annually.
52 Nitro compounds are widely used in industry and nitro groups are key components
53 of numerous biologically active substances such as therapeutics and antibiotics. For
54 example, the antibiotic azomycin and nitroglycerin, which is known as a therapeutic for
55 angina pectoris, both contain nitro groups in their structure [20,21]. Nitroaromatic
56 compounds are also important in industrial contexts. Perhaps the best known
57 nitroaromatic compound is 2,4,6-trinitrotoluene, which is used for explosives, while
58 others such as picric acid, hexanitrostilbene, and hexanitrobenzene are also employed as
59 explosives [22]. Besides such use as explosives, nitroaromatic compounds are also used
60 as starting materials for producing various industrial products, including herbicides and
61 insecticides (e.g., parathion, bifenox, carbofuran) and pharmaceuticals (e.g., the
62 antipsychotic drug phenothiazine synthesized from halonitrobenzene [23]). However, to
63 produce nitroaromatic compounds industrially, direct nitration of aromatic rings is still
64 performed using a mixture of acids (a combination of nitric and sulfuric acids), which is
65 highly hazardous and suffers from difficulties in controlling regioselectivity [24].
66 An alternative method for producing nitroaromatic compounds that has been
67 attracting attention is enzymatic nitration. This approach proceeds under mild
68 conditions and exhibits high regiospecificity. Enzymes that catalyze the synthesis of
69 nitro compounds are relatively rare, but they can be found in a small number of species,
70 including *Streptomyces* sp [24]. A subset of cytochrome P450s have been found to
71 catalyze the direct nitration of aromatic rings for synthesizing nitroaromatic compounds.
72 For instance, TxtE induces nitration at the C4-position of the indole ring of tryptophan

in the biosynthesis of the phytotoxin thaxtomin [25], and RufO introduces a nitro group at the C3-position of the aromatic ring of tyrosine to produce rufomycin [26]. These enzymes synthesize a nitronium ion from a nitric oxide and molecular oxygen to induce nitration of an aromatic ring. Regarding TxtE, several studies have aimed to produce nitrotryptophan using it. For example, Zuo and Ding successfully produced nitrotryptophan *in vivo* by introducing TxtE into *Escherichia coli* [27]. However, it was necessary to introduce not only TxtE but also nitric oxide synthetase. This made the reaction system slightly complicated, so the development of a more convenient system for synthesizing nitroaromatic compounds is anticipated.

As an alternative method of using microbes to synthesize nitro compounds, nitration by oxidation of amino groups using *N*-oxygenase has been identified [24]. For example, CmlI from *Streptomyces venezuelae*, which is involved in the biosynthesis of the well-known antibiotic chloramphenicol [28], and PrnD from *Pseudomonas fluorescens*, which is involved in the biosynthesis of pyrrolnitrin [29], can oxidize an amino group of their substrates. Since *N*-oxygenases utilize molecular oxygens directly to synthesize nitro compounds, it is considered that simpler reaction systems can be applied for synthesizing nitroaromatic compounds using them. In this study, we featured AurF from *Streptomyces thioluteus*, which is involved in the biosynthesis of the antibiotic aureothin [30]. AurF can oxidize an amino group of 4-aminobenzoate (*p*-aminobenzoate: PABA), which is an intermediate of the folate biosynthesis pathway, to synthesize 4-nitrobenzoate (*p*-nitrobenzoate: PNBA). Owing to the broad substrate specificity of AurF [31], AurF has a potential to be applied for synthesizing other natural and/or non-natural nitroaromatic compounds. Studies of AurF conducted to date

have mainly focused on its structure, mechanism of oxidation, and reaction parameters [31-33].

In this study, we attempted to produce PNBA by introducing AurF into *E. coli*. First, during the evaluation of *E. coli* resistance to PNBA, we found that *E. coli* can also degrade it. To identify the genes involved in this degradation, we constructed an *E. coli* strain, which we named PN-1, featuring the disruption of four genes: *nfsA*, *nfsB*, *nemA*, and *azoR*. Our findings confirmed that this strain did not degrade PNBA. We then introduced the *aurF* gene into PN-1, which enabled it to efficiently convert PABA to PNBA. We also found that the overexpression of *pabA*, *pabB*, and *pabC*, which are involved in PABA synthesis, enabled the production of PNBA from glucose. To further improve PNBA production, we disrupted *pheA*, *tyrA*, and *trpE* (PN-2 strain), additionally introduced *pabA*, *pabB*, and *pabC* (PN-3 strain), and disrupted *pykA* and *pykF* (PN-4 strain). Our findings showed that the PN-4 strain could produce 975 mg/L PNBA after 72 h of cultivation. These results should contribute to the microbial production of nitroaromatic compounds.

2. Materials and methods

2.1. Strains and plasmid construction

The strains, plasmids, and primers used in this study are listed in Supplementary Tables S1, S2, and S3, respectively. ATCC31882 and its derivative strain were used for producing PNBA. For gene cloning, NovaBlue competent cells (Novagen, Cambridge, MA, USA) were used. KOD FX Neo (TOYOBO, Osaka, Japan) was used for polymerase chain reaction (PCR). DNA primers were synthesized from Invitrogen Custom DNA Oligos service (Thermo Fisher Scientific, Tokyo, Japan) or DNA Custom

120 Synthesis service (FASMAC, Atsugi, Japan). A codon-optimized foreign gene fragment
121 of *aurF* from *Streptomyces thioluteus* (DDBJ accession number: LC773266) was
122 purchased by Invitrogen GeneArt Gene Synthesis service (Thermo Fisher Scientific).
123 Codon-optimized foreign gene fragments of *pabC* (*OapabC*, *AvpabC*, *SdpabC*, *AppabC*,
124 *XbpabC*) (Genbank accession number: WP_040128554, WP_127051998,
125 WP_011468114, WP_013602677 and WP_038203276, respectively) were synthesized
126 by an Artificial Gene Synthesis service (Twist Bioscience, San Francisco, CA, USA).
127 Plasmids named pZE12-*aurF* and pSAK-*aurF* were prepared as follows. A gene
128 fragment encoding *aurF* was amplified by PCR using the primer pair pZ-*aurF*_Fw and
129 pZ-*aurF*_Rv. The amplified fragments were cloned between the *Kpn* Ⅰ/*Hin*dⅢ site of
130 pZE12MCS or pSAK [34] and the resulting plasmids were designated pZE12-*aurF* and
131 pSAK-*aurF*, respectively.
132 pSAK-*pabABC* was prepared as follows. A *pabA-pabB-pabC* gene fragment was
133 amplified by PCR using pZE12-*pabABC* [35] as a template and the primer pair pZ-
134 *pabABC*_Fw and pZ-*pabABC*_Rv. The amplified fragments were cloned into the *Kpn* Ⅰ
135 /*Hin*dⅢ site of pSAK and the resulting plasmids were designated pSAK-*pabABC*.
136 pZE12-*pabAB* was prepared as follows. A *pabA-pabB* gene fragment was
137 amplified by PCR using pZE12-*pabABC* [35] as a template and the primer pair pZ-
138 *pabAB*_Fw and pZ-*pabAB*_Rv. The amplified fragments were cloned into the *Kpn* Ⅰ
139 /*Hin*dⅢ site of pZE12MCS and the resulting plasmids were designated pZE12-*pabAB*.
140 A plasmid named pZE12-*pabAB-OapabC* was prepared as follows. The *OapabC*
141 gene fragment was amplified by PCR using the primer pair pZ-*OapabC*_Fw and pZ-
142 *OapabC*_Rv. The amplified fragments were cloned into the *Hin*dⅢ site of pZE12-

143 *pabAB* and the resulting plasmid was designated pZE12-*pabAB*-*OapabC*. pZE12-
144 *pabAB*-*AvpabC*, pZE12-*pabAB*-*SdpabC*, pZE12-*pabAB*-*AppabC*, and pZE12-*pabAB*-
145 *XbpabC* were constructed by the same procedure.
146 A plasmid named pTΔ*nfsA* for gene disruption was prepared as follows. A plasmid
147 pTargetF [36] was amplified by PCR with the primer pair del-*nfsA*_Inv_Fw and del-
148 *nfsA*_Inv_Rv. The amplified fragment was self-ligated. The upstream and downstream
149 DNA sequences of *nfsA* were amplified using the primer pair del-*nfsA*_Up_Fw and del-
150 *nfsA*_Up_Rv, del-*nfsA*_Down_Fw, and del-*nfsA*_Down_Rv, with ATCC31882 genomic
151 DNA as the template. The amplified fragments were fused by overlap extension PCR
152 with the primer pair del-*nfsA*_Up_Fw and del-*nfsA*_Down_ Rv. The fused fragments
153 were cloned into the *Eco*R Ⅰ/*Hin*dⅢ sites of the plasmids self-ligated earlier and the
154 resulting plasmids were designated pTΔ*nfsA*. pTΔ*nfsB*, pTΔ*nemA*, and pTΔ*azoR* were
155 constructed by the same procedure.
156 pTΔ*azoR*::$P_{A1lacO-1}$-*pabABC* was constructed as follows. pSAK-*pabABC* was
157 amplified by PCR with the primer pair *azoR*_lac_Fw and *azoR*_lac_Rv. The amplified
158 fragments were cloned into the *Spe*I sites of pTΔ*azoR*, and the resulting plasmid was
159 designated pTΔ*azoR*::$P_{A1lacO-1}$-*pabABC*.
160 Disruption of *nfsA*, *nfsB*, *nemA*, *azoR*, *pheA*, *tyrA*, *trpE*, *pykA*, and *pykF* and
161 transduction of *pabABC* were performed using the CRISPR-Cas9-plasmid system [36]
162 with pTΔ*nfsA*, pTΔ*nfsB*, pTΔ*nemA*, pTΔ*azoR*, pTΔ*pheA*, pTΔ*tyrA*, pTΔ*trpE*, pTΔ*pykA*,
163 pTΔ*pykF*, and pTΔ*azoR*::$P_{A1lacO-1}$-*pabABC*. A host strain introduced with pCas and
164 pTarget (e.g.,pTΔ*nfsA*) was cultivated in 2×YT medium with 30 mM L-arabinose
165 overnight and the solution was spread on the LB plate. After overnight incubation, each

colony was checked by colony PCR with corresponding check primers (e.g., del-*nfsA*_Check_Fw, del-*nfsA*_Check_Rv) if the disruption was succeeded.

pZE12-*pabAB*-*pabC*^{F26ram} was constructed as follows. pZE12-*pabABC* was amplified by PCR with the primer pair PabC_F26ram_Fw and PabC_F26ram_Rv. The amplified fragment was self-ligated. Other plasmids for PabC mutation were constructed by the same procedure.

2.2. Medium

LB medium was used for pre-culture and culture for genetic manipulation. This medium consisted of 10 g/L tryptone, 5 g/L yeast extract, and 5 g/L NaCl. M9Y medium was used for PNBA production. This medium contained 20 g/L glucose, 5 g/L yeast extract, 17.1 g/L $Na_2HPO_4 \cdot 12H_2O$, 3 g/L KH_2PO_4, 1 g/L NH_4Cl, 1 mM $MgSO_4 \cdot 7H_2O$, 0.1 mM $CaCl_2 \cdot 2H_2O$, 0.01 mM $FeSO_4 \cdot 7H_2O$, 10 mg/L thiamine hydrochloride, and 0.1 mM IPTG, and 100 mg/L ampicillin and/or 30 mg/L chloramphenicol were added if needed. Sodium pyruvate (1 g/L) was added during PN-4 strain cultivation. 2×YT medium consisted of 16 g/L tryptone, 10 g/L yeast extract, and 5 g/L NaCl.

2.3. Cultivation conditions

Colonies of *E. coli* from LB plates were inoculated into test tubes with 5 mL of LB medium and incubated at 37 °C and 220 rpm, overnight. The pre-culture solution was then inoculated into test tubes containing 5 mL of M9Y medium to initial OD_{600} = 0.05 and incubated at 37 ℃ and 220 rpm. For analyses of bacterial cell growth and metabolites, 400 μL of the solution was collected and centrifuged at 10,000 rpm for 10 min. The supernatant was analyzed by high performance liquid chromatography

(HPLC). To test PNBA toxicity, PNBA (adjusted to pH 7) was added after 8 h of cultivation. For evaluation of PabC mutants, PNBA (adjusted to pH 7) was added after 8 h of cultivation and sample were collected after 24 h cultivation.

2.4. Analytical methods

Bacterial cell growth was evaluated by measuring the optical density at 600 nm with a UVmini-1240 spectrophotometer (Shimadzu Corporation, Kyoto, Japan). For PABA and PNBA analyses, HPLC (Shimadzu Corporation) equipped with an MS Ⅱ column (5 μm, 4.6 mm I.D. ×250 mm L; Nacalai Tesque) was used. HPLC profiles were obtained using a 254 nm UV-VIS detector. The two-component system was used and the mobile phase was A 0.2% phosphate buffer and B methanol. The gradient was started with a 70:30 mixture of A and B, and shifted to a 50:50 mixture gradually from 4 min, with this ratio being retained from 6 to 14 min. It was then returned to a 70:30 mixture at 16 min. The flow rate of the mobile phase was 1.0 mL/min and the column remained at 40 °C. For glucose analysis, prominence HPLC (Shimadzu Corporation) equipped with a Shodex SUGAR KS-801 column (6 μm, 8.0 mm I.D. ×300 mm L; Shodex) was used. The mobile phase was water and HPLC profiles were obtained using a refractive index detector. The flow rate was 0.8 mL/min and the column was maintained at 50 °C.

3. Results

3.1. Evaluation of PNBA toxicity for *E. coli*

Nitroaromatic compounds are typically toxic to living organisms [37]. First, we evaluated the toxicity of PNBA to *E. coli* prior to attempting to produce PNBA using it.

The CFT1 strain was selected as the host due to its reported suitability for producing aromatic compounds [35]. To prevent contamination, CFT1 introduced with pZE12MCS (CFT1e), which is resistant to ampicillin, was used in this experiment. PNBA was added to M9Y medium at concentrations of 0.5, 1.5, 3, and 7 g/L 8 h after cultivation. Contrary to expectations, the bacterial cell growth was improved at PNBA concentrations of 0.5, 1.5, and 3 g/L (Figure 1A). Meanwhile, in the presence of 7 g/L PNBA, the cell growth was mostly inhibited. Upon analyzing the culture medium, we found that the PNBA concentration had decreased (Figure 1B), indicating that PNBA had been degraded. We incubated the medium containing 0.5 g/L PNBA with or without CFT1e (medium only). After 24 h, no PNBA was detected in the medium with CFT1e, whereas almost all PNBA remained in the medium without CFT1e fermentation (Supplementary Figure S1). This provided evidence that *E. coli* can degrade PNBA.

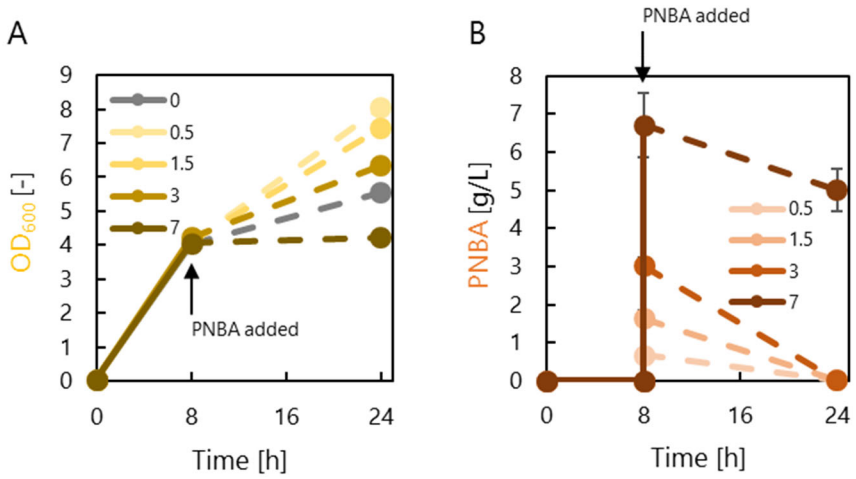

Figure 1. Bacterial tolerance of CFT1e resulted from the addition of 0.5, 1.5, 3, and 7 g/L PNBA at 8 h after cultivation. (A) Bacterial cell growth. **(B)** The PNBA concentrations in culture supernatants. The time when PNBA was added is indicated by arrows. The data are shown as means of three independent experiments with standard deviations.

3.2. Identifying genes related to PNBA degradation

To prevent PNBA degradation, we aimed to identify the genes involved in this process. No reports have been published on the disassembly of PNBA by *E. coli*, to the best of our knowledge. However, several genes involved in the reduction of nitro compounds have been reported. First, we focused on the genes *nfsA* and *nfsB* encoding nitro reductases. NfsA and NfsB are known as a major nitro reductase and a minor nitro reductase, respectively, and they have been reported to reduce a variety of nitro compounds, including PNBA [38, 39]. Thus, we disrupted these two genes in CFT1, which produced strain CFT1ΔAB, and carried out the PNBA degradation experiment. Then, CFT1ΔABe, a strain harboring an empty vector, degraded only about 40% of the PNBA added, while CFT1e (a strain harboring empty vector) degraded all PNBA added at 24 h (Figure 2). This indicated the involvement of other genes in PNBA degradation. Therefore, we next disrupted *nemA*, which is known to be involved in degrading trinitrotoluene (TNT). A previous study showed that *E. coli* with disruption of all of *nfsA*, *nfsB*, and *nemA* does not completely degrade TNT [40]. Furthermore, we deleted *azoR*, the gene encoding azo reductase, which was found to reduce a nitroaromatic prodrug [41]. When these two genes, *nemA* and *azoR*, of CFT1ΔAB were disrupted, the resulting strain PN-1e hardly degraded PNBA (Figure 2).

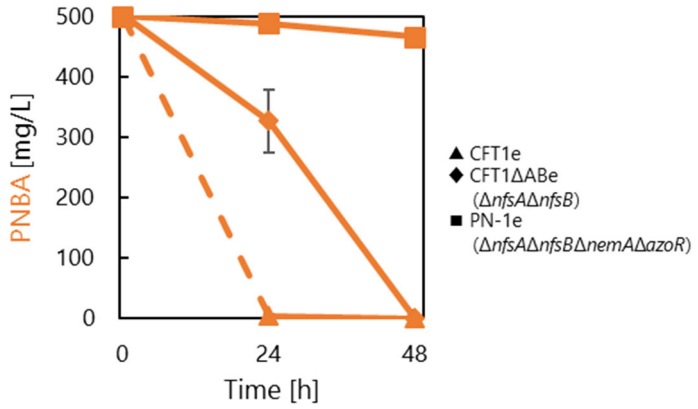

Figure 2. The PNBA concentration during the cultivation of CFT1e, CFT1ΔABe, and PN-1e. The data are shown as means of three independent experiments with standard deviations.

3.3. Conversion from PABA to PNBA by AurF

The findings showed that the PN-1 strain does not degrade PNBA, leading us to attempt PNBA production within this strain. We introduced the *aurF* gene originating from *Streptomyces thioluteus* into PN-1 and CFT1 strains; however, the resultant strains PN-1a and CFT1a did not produce PNBA (data not shown). Although *E. coli* can produce the precursor PABA, it can only do so in limited quantities. Therefore, we added PABA to the medium to test the function of AurF (Figure 3A). PN-1a could produce 375 mg/L PNBA in the medium containing 1 g/L PABA at 48 h (Figure 3B), which is a higher yield than that produced by CFT1a (60 mg/L).

This suggested that PN-1 is more suitable for producing PNBA than CFT1, but almost half of the PABA added remained, suggesting that there is room for improvement of the reaction by AurF. Thus, we changed the *aurF* expression system from a high-copy vector (pZE12MCS) to a low-copy one (pSAK). PN-1 carrying

pSAK-*aurF* (PN-1A) could produce 945 mg/L PNBA from 1 g/L PABA after 48 h (Figure 3B). The cell growth of PN-1A was also superior to that of PN-1a (Figure 3C).

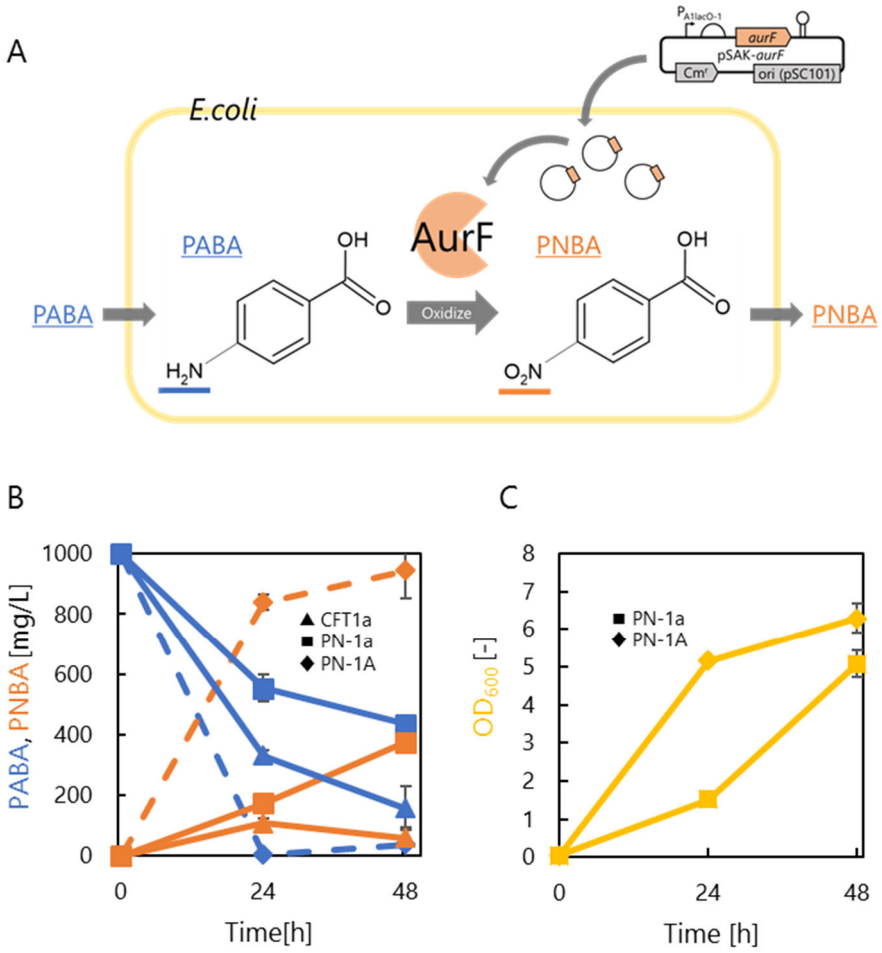

Figure 3. PNBA production from PABA. (A) Schematic illustration of PABA production. The conversion of PABA to PNBA by AurF-expressing *E. coli* was evaluated through the addition of PABA to the growth medium. **(B)** Time courses of PABA and PNBA. Here, 1 g/L PABA (1 g/L) was initially added to the medium during the cultivation of CFT1a, PN-1a, and PN-1A. The concentrations of PABA and PNBA are shown in blue and orange, respectively. **(C)** Cell growth of PN-1a and PN-1A. The data are shown as means of three independent experiments with standard deviations.

3.4. PNBA production from glucose by overexpressing *pabABC*

We successfully engineered a strain capable of converting PABA to PNBA, and subsequently proceeded to use it to directly produce PNBA from glucose. To achieve this, the *E. coli pabA*, *pabB*, and *pabC* genes were overexpressed in PN-1A (Figure 4A). These genes are involved in the PABA synthesis from chorismate, an important intermediate of the aromatic amino acid biosynthetic pathway. PabA and PabB convert chorismate to 4-amino-4-deoxychorismate by replacing a hydroxy group with an amino group, and PabC releases pyruvate, resulting in the formation of PABA [42-44]. These genes were overexpressed in PN-1A using a high-copy plasmid. The resultant strain PN-1Ap successfully produced 393 mg/L PNBA after 72 h in M9Y medium with 20 g/L glucose (Figure 4B). Although the titer of PNBA increased over time, no PABA accumulation was detected (Figure 4B). This implies that AurF worked well, while the carbon flux to PABA needed to be enhanced to increase PNBA production.

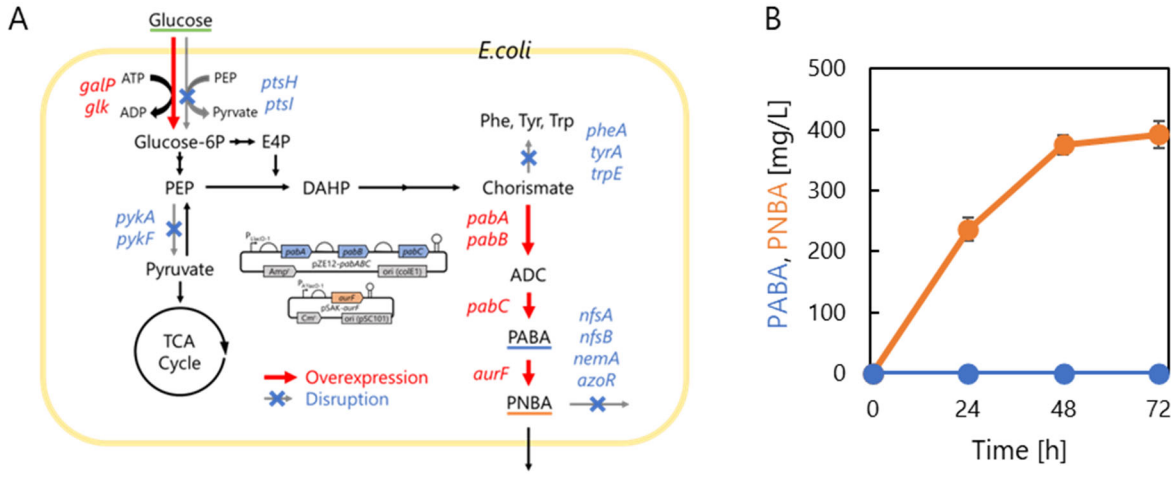

Figure 4. PNBA production from glucose. (A) Metabolic engineering of PNBA-producing *E. coli*. G6P, glucose 6-phosphate; E4P, erythrose 4-phosphate; PEP, phosphoenolpyruvate; DAHP, 3-deoxy-D-arabinoheptulosonic acid 7-phosphate; ADC, 4-amino-4-deoxychorismate; PABA, *p*-aminobenzoate; PNBA, *p*-nitrobenzoate; *galP*,

298 D-galactose transporter; *glK*, glucokinase; *ptsH*, phosphocarrier protein Hpr; *ptsI*,
299 phosphoenolpyruvate-protein phosphotransferase; *pykA*, pyruvate kinase; *pykF*,
300 pyruvate kinase; *pheA*, chorismate mutase/prephenate dehydratase; *tyrA*, chorismate
301 mutase/prephenate dehydrogenase; *trpE*, anthranilate synthase component; *pabA*, *p*-
302 aminobenzoate synthetase component; *pabB*, *p*-aminobenzoate synthetase component;
303 *pabC*, 4-amino-4-deoxychorismate lyase; *aurF*, *p*-aminobenzoate *N*-oxygenase from
304 *Streptomyces thioluteus*. **(B)** Culture profiles of PN-1Ap in M9Y medium containing 20
305 g/L glucose. The titers of PABA and PNBA are shown in blue and orange, respectively.
306 The data are shown as means of three independent experiments with standard
307 deviations.
308
309 **3.5. Metabolic engineering for increasing carbon flux to PABA**
310 The endogenous phosphotransferase system (PTS) of the host strain, PN-1 derived
311 from CFT1, was replaced with a galactose permease/glucokinase system (GalP/Glk
312 system) to enhance the availability of phosphoenolpyruvate (PEP), a crucial starting
313 substrate for the shikimate pathway [35]. CFT1 strain was constructed by
314 simultaneously disrupting *ptsHI* of ATCC31882 strain and introducing *glK-galP* by
315 using Quick & Easy *E.coli* Gene Deletion Kit. CFT1 is able to convert glucose to
316 glucose 6-phosphate with ATP, not PEP, resulting saving PEP for aromatic compounds
317 production. Strains derived from CFT1 showed great ability of producing some
318 aromatic compounds (salicylate, 4-hydroxybenzoate, 3-hydroxybenzoate, 2-
319 hydroxybenzoate, 4-aminobenzoate, L-tyrosine, phenol) [35]. To increase the
320 accumulation of the important precursor chorismate, we generated strain PN-2 by
321 disrupting *pheA*, *tyrA*, and *trpE* of the PN-1 strain. These genes are involved in

synthesis of the aromatic amino acids phenylalanine, tyrosine, and tryptophan, respectively, from chorismate. When PN-2Ap was cultivated, the PNBA concentration was increased to 680 mg/L after 72 h of cultivation (Figure 5), which is about 1.7-fold higher than that of PN-1Ap. Moreover, when only *pabA*, *pabB* and *pabC* were overexpressed in PN-2 (PN-2p), it produced more PABA than PN-1p (Supplementary Figure S2). This outcome demonstrates that enhancing the PABA production ability leads to an increase in PNBA production. Subsequently, the PN-3 strain was created by integrating the *pabA*, *pabB*, and *pabC* genes into the genome to enhance their expression. PN-3Ap produced more PNBA (850 mg/L after 72 h) than PN-2Ap. Finally, strain PN-4 was generated by deleting *pykA* and *pykF* from the PN-3 strain. PykA and PykF are involved in the conversion of phosphoenolpyruvate (PEP) to pyruvate. PN-4Ap produced 975 mg/L PNBA, which is 1.2-fold higher than that of PN-3Ap (Figure 5). Notably, almost no PABA accumulated in any strain that we constructed. It was suggested that the carbon flux to PABA remained insufficient, for which further improvements were needed.

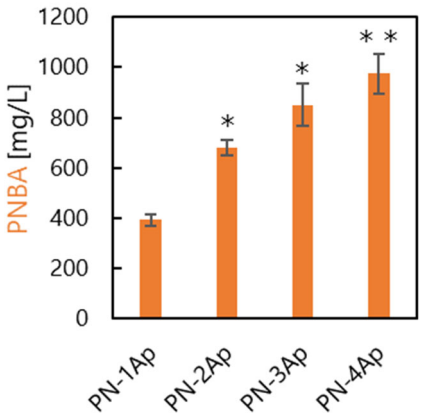

Figure 5. PNBA production after 72 h of cultivation in M9Y medium. The data are shown as means of three independent experiments with standard deviations. *$p < 0.05$, **$p < 0.01$ compared with PN-1Ap.

3.6. Inhibition of PABA synthesis by PNBA

PABA synthesis is crucial for PNBA production. Therefore, we evaluated PABA production with the PN-4p strain, which overexpressed *pabA*, *pabB*, and *pabC*. We found that PN-4p produced 2.46 g/L PABA, which is approximately 2.5 times higher than the PNBA production by PN-4Ap (Figure 6A). Given that all PABA is converted to PNBA, the amount of PNBA produced by PN-4Ap is lower than expected. In addition, the glucose consumption of PN-4Ap was 10 g/L (Figure 6B), which was less than that of PN-4p. Moreover, cell growth of PN-4Ap was slightly lower than that of PN-4p (Figure 6C). From these findings, we hypothesized that the PNBA produced may negatively impact the synthesis of PABA.

To test this hypothesis, we added PNBA to the culture medium of the PN-1p strain at 8 h (Figure 6D–F). The results showed that the production of PABA decreased by less than half in the presence of PNBA (Figure 6D). No significant difference was observed in glucose consumption (Figure 6E) or cell growth (Figure 6F) after 24 h, suggesting that the presence of PNBA inhibited PABA synthesis.

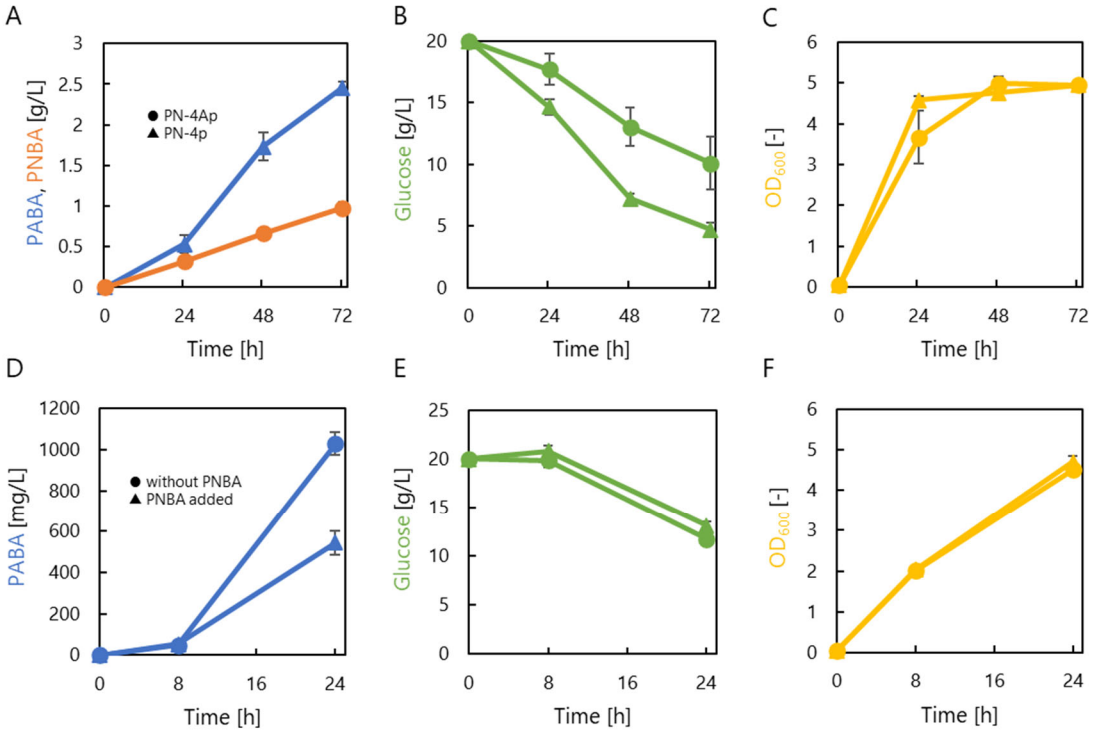

Figure 6. Inhibition of PABA synthesis by PNBA. Culture profiles of PN-4Ap (circles; PNBA-producing strain) and PN-4p (triangles; PABA-producing strain) in M9Y medium containing 20 g/L glucose. **(A)** Concentrations of PABA and PNBA. **(B)** Glucose consumption. **(C)** Cell growth. Panels. **(D–F)** show culture profiles of PN-1p in M9Y medium with/without adding 0.5 g/L PNBA at 8 h after cultivation. **(D)** Concentrations of PABA and PNBA. **(E)** Glucose consumption. **(F)** Cell growth. The data are shown as means of three independent experiments with standard deviations.

4. Discussion

In this study, we achieved the successful production of PNBA from glucose for the first time by employing *E. coli* utilizing AurF. Initially, we identified the genes involved in degrading PNBA in *E. coli*. After tuning the *aurF* expression system, we obtained a strain that efficiently synthesizes PNBA from PABA. Subsequently, via the

371 overexpression of *pabA*, *pabB, pabC*, and *aurF*, we achieved the production of PNBA
372 from glucose. Then, via metabolic engineering to enhance the flux to PABA, we
373 increased the PNBA titer of PN-4Ap to 975 mg/L in 72 h, which is about 2.5 times
374 higher than that of the starting strain (PN-1Ap).
375 The host strain CFT1 exhibited the ability to degrade PNBA, but after disrupting
376 four genes, namely, *nfsA*, *nfsB*, *nemA*, and *azoR*, the resulting strain PN-1 lost its ability
377 to degrade PNBA. Nitroreductases are known to degrade nitroaromatic compounds,
378 forming hydroxyl amino or nitroso groups, and amino groups [45]. The biodegradation
379 pathway of PNBA has been previously reported in *Burkholderia cepacia* and *Ralstonia*
380 *paucula* [46]. It suggests that PNBA is predominantly reduced to 4-
381 hydroxylaminobenzoate, which can then be converted to 3-hydroxy-4-aminobenzoate or
382 protocatechuate, and that the pathway leading to PABA is minor. Our findings show that
383 PABA was detected after CFT1e was cultivated in the presence of PNBA; however, the
384 amount of PABA detected was less than expected based on the amount of PNBA
385 consumed (Supplementary Figure S3). These results suggest that *E. coli* appears to
386 degrade PNBA in a manner similar to that observed in previous studies.
387 As shown in Figure 3B, CFT1a consumed more PABA than PN-1a, despite
388 producing less PNBA. This seems to be paradoxical, but it is reasonable considering
389 that CFT1a degraded PNBA that it produced itself. In the case of PN-1a, the PNBA titer
390 was supposed to correspond to the PABA consumption. However, PN-1a consumed 565
391 mg/L (4.13 mM) PABA at 48 h and produced only 375 mg/L (2.44 mM). This is
392 attributed to the reaction of PABA with the medium. A previous study demonstrated that
393 PABA reacts with glucose and forms a glycated product [47]. The same reaction is
394 considered to have occurred in the present study. Interestingly, contrary to the

395 expectation that higher expression of AurF would lead to a higher titer, PNBA
396 production from PABA was improved by using a low-copy vector (Figure 3B). The
397 copy number of pZE12 (ori: colE1) is about 70-100 and that of pSAK (ori: pSC101) is
398 10-15 [48]. Therefore, low-level AurF expression is better than high-level expression.
399 We also observed that, although *E. coli* was relatively tolerant of PNBA (Figure 1A),
400 the addition of PNBA to the medium at the beginning of cultivation impeded the cell
401 growth more severely (Supplementary Figure S4). These findings suggest that excessive
402 PNBA production in the early stage of cultivation inhibited bacterial cell growth in PN-
403 1a, whereas PN-1A could maintain a balance between cell growth and PNBA
404 production. In addition, the high enzymatic activity of AurF *in vitro*, as reported by
405 Chanco et al. (1.99 ± 0.27 μmol/mg/min), may have contributed to the efficient PNBA
406 production even when a low-copy vector was used [31].
407 The bottleneck of PNBA production from glucose was identified as the step
408 involving PABA synthesis. The production of PABA using various organisms has been
409 attempted, with notable examples being *Saccharomyces cerevisiae*, *E. coli*, and
410 *Corynebacterium glutamicum*. As for *S. cerevisiae*, Averesch et al. reported the
411 production of 215 mg/L PABA (yield 2.64%) from glycerol and ethanol as carbon
412 sources [49]. They disrupted *ARO7* and *TRP3*, which are involved in aromatic amino
413 acid synthesis, and overexpressed *ABZ1* and *ABZ2*, which have the same functions as
414 *pabAB* and *pabC*, respectively, from wine yeasts. For *E. coli*, Koma et al. reported the
415 production of 700 mg/L PABA from 10 g/L glucose (yield 0.09 mol/mol) in a test tube,
416 by overexpressing the feedback-resistant 3-deoxy-D-arabino-heptulosonate-7-phosphate
417 (DAHP) synthase $aroF^{fbr}$ and *pabAB* from *Corynebacterium efficiens*, resulting in
418 redirecting the chorismate flow to PABA from phenylalanine and tyrosine [50]. In this

419 study, we aimed to increase the carbon flux toward PABA by overexpressing *pabA*,
420 *pabB*, and *pabC*, disrupting the phenylalanine-, tyrosine-, and tryptophan-producing
421 pathways, and deleting *pykA* and *pykF*. The resulting strain PN-4p produced 2.46 g/L
422 PABA with a yield of 0.16 mol/mol, which is higher than in these previous studies. In
423 the case of *Corynebacterium glutamicum*, Kubota et al. reported the production of 6.2
424 g/L PABA from glucose in a test tube [47].They screened *pabAB* and *pabC* genes from
425 other microorganisms and found that the combination of *pabAB* from *Corynebacterium*
426 *callunae* and *pabC* from *Xenorhabdus bovienii* was most effective. We also evaluated
427 these *pabC* genes, but none of them outperformed *pabC* from *E. coli* (Supplementary
428 Figure S5).
429 In this study, we focused on AurF, an oxidizing enzyme targeting an amino group
430 of PABA. AurF is known to have broad substrate specificity [31, 51] compared with
431 other *N*-oxygenases such as PrnD [52] and CmlI [24]. AurF can accept compounds with
432 substitution at the 2' or 3' position and compounds with the replacement of carboxylate
433 by other groups such as methyl carboxylate and nitro groups. In addition, AurF can
434 induce nitration of the *m*-substituted substrate, although its activity is significantly
435 lower than that of PABA. Given its broad substrate specificity, AurF holds potential for
436 the production of other nitroaromatic compounds. It will represent a novel strategy for
437 synthesizing non-natural compounds. However, as the product structure closely
438 resembles the substrate, enzyme inhibition is possible, as evidenced by our results
439 (Figure 6). Inhibitions due to products have been observed in microbial production. For
440 example, the genes *aroG* and *aroF* encoding DAHP synthases were shown to receive
441 feedback inhibition by phenylalanine and tyrosine, respectively. However, these
442 enzymes have been engineered to be insensitive to their own products by certain single

mutations. We attempted to construct a PabC mutant that would not be inhibited by PNBA by introducing mutations at various sites of PabC (F26, T27, A29, R30, L53, R90, G91, I135, I139, K140, H141, N143, R144, L145, G196, V197, N198, G199, I200, C235), but none of them exhibited improved PNBA titer (data not shown).

In conclusion, we achieved one of the nitroaromatic compounds PNBA production from glucose by introducing the gene AurF into *E.coli* and found that the bottleneck of PNBA production is the step of synthesizing PABA. Our findings should contribute to the microbial production for nitroaromatic compounds.

CRediT authorship contribution statement

Ayana Mori: Conceptualization, Investigation, and Writing - original draft. **Yuuki Hirata:** Investigation. **Mayumi Kishida:** Investigation. **Yutaro Mori:** Data curation, Writing - review and editing. **Akihiko Kondo:** Resources. **Shuhei Noda:** Data curation, Writing - review & editing. **Tsutomu Tanaka:** Conceptualization, Writing - review & editing, Funding acquisition, Project administration.

Declaration of competing interest

The authors declare no competing financial interests.

Acknowledgements

This work was supported by Japan Society for the Promotion of Science (JSPS) Grants-in-Aid for Scientific Research (B) (Grant Number 22H01880) and (A) (Grant Number 20H00321), and the Sumitomo Foundation (to T.T.).The authors would like to thank Enago (www.enago.jp) for the English language review.

References

[1] Liu, Y., Cruz-Morales, P., Zargar, A., Belcher, M. S., Pang, B., Englund, E., Dan, Q., Yin, K., Keasling, J. D. Biofuels for a sustainable future. *Cell*. *184* (6) (2021), 1636–1647.

[2] Liu, Z., Wang, J., Nielsen, J. Yeast synthetic biology advances biofuel production. *Curr Opin Microbiol*. *65* (2022), 33–39.

[3] Biggs, B. W., Alper, H. S., Pfleger, B. F., Tyo, K. E. J., Santos, C. N. S., Ajikumar, P. K., Stephanopoulos, G. Enabling commercial success of industrial biotechnology. *Science*. *374* (6575) (2021), 1563–1565.

[4] Song, C. W., Park, J. M., Chung, S. C., Lee, S. Y., Song, H. Microbial production of 2,3-butanediol for industrial applications. *J Ind Microbiol Biotechnol. 46* (11) (2019), 1583–1601.

[5] Liang, P., Cao, M., Li, J., Wang, Q., Dai, Z, 2023. Expanding sugar alcohol industry: Microbial production of sugar alcohols and associated chemocatalytic derivatives. *Biotechnol Adv. 64*, 108105.

[6] Gupta, M., Wong, M., Jawed, K., Gedeon, K., Barrett, H., Bassalo, M., Morrison, C., Eqbal, D., Yazdani, S. S., Gill, R. T., Huang, J., Douaisi, M., Dordick, J., Belfort, G., Koffas, M. A. G, 2022. Isobutanol production by combined in vivo and in vitro metabolic engineering. *Metab Eng Commun. 15,* e00210.

[7] Trichez, D., Carneiro, C. V. G. C., Braga, M., Almeida, J. R. M. Recent progress in the microbial production of xylonic acid. *World J Microbiol Biotechnol*. *38* (2022), 127.

[8] Li, J., Rong, L., Zhao, Y., Li, S., Zhang, C., Xiao, D., Foo, J. L., Yu, A, 2020. Next-generation metabolic engineering of non-conventional microbial cell factories for carboxylic acid platform chemicals. *Biotechnol Adv*. *43*, 107605.

[9] Ahn, J. H., Seo, H., Park, W., Seok, J., Lee, J. A., Kim, W. J., Kim, G. B., Kim, K. J., Lee, S. Y. Enhanced succinic acid production by mannheimia employing optimal malate dehydrogenase. *Nat Commun. 11* (2020), 1970.

[10] Chae, T. U., Ahn, J. H., Ko, Y. S., Kim, J. W., Lee, J. A., Lee, E. H., Lee, S. Y. Metabolic engineering for the production of dicarboxylic acids and diamines. *Metab Eng*. *58* (2020), 2–16.

[11] Tran, V. G., Zhao, H, 2022. Engineering robust microorganisms for organic acid production. *J Ind Microbiol Biotechnol*. *49* (2), kuab067.

[12] Sun, L., Gong, M., Lv, X., Huang, Z., Gu, Y., Li, J., Du, G., Liu, L. Current advance in biological production of short-chain organic acid. *Appl Microbiol Biotechnol*. 104 (21) (2020), 9109–9124.

[13] Jovanovic, S., Dietrich, D., Becker, J., Kohlstedt, M., Wittmann, C. Microbial production of polyunsaturated fatty acids — high-value ingredients for aquafeed, superfoods, and pharmaceuticals. *Curr Opin Biotechnol*. *69* (2021), 199–211.

[14] Hirasawa, T., Shimizu, H. Recent advances in amino acid production by microbial cells. *Curr Opin Biotechnol*. *42* (2016), 133–146.

[15] Shen, Y. P., Niu, F. X., Yan, Z. B., Fong, L. S., Huang, Y. Bin, Liu, J. Z. Recent advances in metabolically engineered microorganisms for the production of aromatic chemicals derived from aromatic amino acids. *Front Bioeng Biotechnol*. *8* (2020), 407.

[16] Vo, T. M., Park, S. Metabolic engineering of escherichia coli w3110 for efficient production of homoserine from glucose. *Metab Eng*. *73* (2022), 104–113.

[17] Yu, S., Zheng, B., Chen, Z., Huo, Y. X. Metabolic engineering of corynebacterium glutamicum for producing branched chain amino acids. *Microb Cell Fact*. *20* (2021), 230.

[18] Wendisch, V. F. Metabolic engineering advances and prospects for amino acid production. *Metab Eng*. *58* (2020), 17–34.

[19] Yuan, S. F., Nair, P. H., Borbon, D., Coleman, S. M., Fan, P. H., Lin, W. L., Alper, H. S. Metabolic engineering of E. coli for β-alanine production using a multi-biosensor enabled approach. *Metab Eng*. *74* (2022), 24–35.

[20] Osato, T., Ueda, M., Fukuyama, S, Yagishita K., Okami, Y., Umezawa, H. Production of tertiomycin (a new antibiotic substance), azomycin and eurocidin by S. eurocidicus. *J Antibiot A. 8* (1955), 105–109.

[21] Divakaran, S., Loscalzo, J. The role of nitroglycerin and other nitrogen oxides in cardiovascular therapeutics. *J Am Coll Cardiol*. *70* (19) (2017), 2393–2410.

[22] Ju, K.-S., Parales, R. E. Nitroaromatic compounds, from synthesis to biodegradation. *Microbiol Mol Biol Rev. 74* (2) (2010), 250–272.

[23] Gritsenko, A. N., Ermakova, Z. I., Zhuravlev, S. V. Synthesis in the phenothiazine series. *Chem Heterocycl Compd*. *6* (1970), 1245–1246

[24] Nóbile, M. L., Stricker, A. M., Marchesano, L., Iribarren, A. M., Lewkowicz, E. S. N-oxygenation of amino compounds: early stages in its application to the biocatalyzed preparation of bioactive compounds. *Biotechnol Adv*. *51* (2021), 107726

[25] Barry, S. M., Kers, J. A., Johnson, E. G., Song, L., Aston, P. R., Patel, B., Krasnoff, S. B., Crane, B. R., Gibson, D. M., Loria, R., Challis, G. L. Cytochrome p450-catalyzed l-tryptophan nitration in thaxtomin phytotoxin biosynthesis. *Nat Chem Biol*. *8* (10) (2012), 814–816.

[26] Tomita, H., Katsuyama, Y., Minami, H., Ohnishi, Y. Identification and characterization of a bacterial cytochrome p450 monooxygenase catalyzing the 3-nitration of tyrosine in rufomycin biosynthesis. *J Bioll Chem. 292* (38) (2017), 15859–15869.

[27] Zuo, R., Ding, Y. Direct aromatic nitration system for synthesis of nitrotryptophans in Escherichia coli. *ACS Synth Biol*. *8* (4) (2019), 857–865.

[28] Lu, H., Chanco, E., Zhao, H. CmlI is an N-oxygenase in the biosynthesis of chloramphenicol. *Tetrahedron*. *68* (37) (2012), 7651–7654.

[29] Lee, J. K., Ang, E. L., Zhao, H. Probing the substrate specificity of aminopyrrolnitrin oxygenase (PrnD) by mutational analysis. *J Bacteriol. 188* (17) (2006), 6179–6183.

[30] He, J., Hertweck, C. Biosynthetic origin of the rare nitroaryl moiety of the polyketide antibiotic aureothin: involvement of an unprecedented N-oxygenase. *J Am Chem Soc. 126* (12) (2004), 3694–3695.

[31] Chanco, E., Choi, Y. S., Sun, N., Vu, M., Zhao, H. Characterization of the N-oxygenase AurF from Streptomyces thioletus. *Bioorg Med Chem. 22* (20) (2014), 5569–5577.

[32] Seong Choi, Y., Zhang, H., Brunzelle, J. S., Nair, S. K., Zhao, H. In vitro reconstitution and crystal structure of p-aminobenzoate N-oxygenase (AurF) involved in aureothin biosynthesis. *Proc Natl Acad Sci U S A*. *105* (19) (2008), 6858–6863.

[33] Li, N., Korboukh, V. K., Krebs, C., Bollinger, J. M. Four-electron oxidation of p-hydroxylaminobenzoate to p-nitrobenzoate by a peroxodiferric complex in AurF from Streptomyces thioluteus. *Proc Natl Acad Sci U S A*. *107* (36) (2010), 15722–15727.

[34] Fujiwara, R., Noda, S., Tanaka, T., Kondo, A. Metabolic engineering of escherichia coli for shikimate pathway derivative production from glucose–xylose co-substrate. *Nat Commu. 11* (1) (2020), 279.

[35] Noda, S., Shirai, T., Oyama, S., Kondo, A. Metabolic design of a platform Escherichia coli strain producing various chorismate derivatives. *Metab Eng. 33* (2016), 119–129.

[36] Jiang, Y., Chen, B., Duan, C., Sun, B., Yang, J., Yang, S. Multigene editing in the Escherichia coli genome via the CRISPR-Cas9 System. *Appl Environ Microbiol. 81* (7) (2015), 2506–2514.

[37] Kovacic, P., Somanathan, R. Nitroaromatic Compounds: Environmental Toxicity, Carcinogenicity, Mutagenicity, Therapy and Mechanism. *J Appl Toxicol. 34* (8) (2014), 810–824.

[38] Zenno, S., Koike, H., Kumar, A. N., Jayaraman, R., Tanokura, M., Saigo, K. Biochemical characterization of NfsA, the Escherichia coli major nitroreductase exhibiting a high amino acid sequence homology to frp, a vibrio harveyi flavin oxidoreductase. *J Bacteriol. 178* (1996), 4508–4514.

[39] Zenno, S., Koike, H., Tanokura, M., Saigo, K. Gene cloning, purification, and characterization of NfsB, a minor oxygen-insensitive nitroreductase from Escherichia coli, similar in biochemical properties to FRase I, the major flavin reductase in Vibrio fischeri. *J Biochem. 120* (4) (1996), 736–744.

[40] González-Pérez, M. M., Van Dillewijn, P., Wittich, R. M., Ramos, J. L. Escherichia coli has multiple enzymes that attack TNT and release nitrogen for growth. *Environ Microbiol. 9* (6) (2007), 1535–1540.

[41] Prosser, G. A., Copp, J. N., Syddall, S. P., Williams, E. M., Smaill, J. B., Wilson, W. R., Patterson, A. V., Ackerley, D. F. Discovery and evaluation of Escherichia coli nitroreductases that activate the anti-cancer prodrug CB1954. *Biochem Pharmacol 79* (5) (2010), 678–687.

[42] Tran, P. v, Bannor, T. A., Doktor, S. Z., Nichols, B. P. chromosomal organization and expression of Escherichia coli PabA. *J Bacteriol. 172* (1) (1990), 397–410.

[43] Green, J. M., Merkel, W. K., Nichols, B. P. Characterization and sequence of Escherichia coli PabC, the gene encoding aminodeoxychorismate lyase, a pyridoxal phosphate-containing enzyme. *J Bacteriol. 174* (16) (1992), 5317–5323.

[44] Ye, Q. Z., Liu, J., Walsh, C.T. p-Aminobenzoate synthesis in Escherichia coli: purification and characterization of PabB as aminodeoxychorismate synthase and enzyme X as aminodeoxychorismate lyase. *Proc Natl Acad U S A. 87* (23) (1990), 9391–9395.

[45] Roldán, M. D., Pérez-Reinado, E., Castillo, F., Moreno-Vivián, C. Reduction of polynitroaromatic compounds: the bacterial nitroreductases. *FEMS Microbiol Rev. 32* (3) (2008), 474–500.

[46] Peres, C. M., Russ, R., Lenke, H., Agathos, S. N. Biodegradation of 4-nitrobenzoate, 4-aminobenzoate and their mixtures: new strains, unusual

608 metabolites and insights into pathway regulation. *FEMS Microbiol Ecol. 37* (2)
609 (2006), 151–159.
610 [47] Kubota, T., Watanabe, A., Suda, M., Kogure, T., Hiraga, K., Inui, M. Production
611 of para-aminobenzoate by genetically engineered Corynebacterium glutamicum
612 and non-biological formation of an n-glucosyl byproduct. *Metab Eng. 38* (2016),
613 322–330.
614 [48] Thompson, M. G., Sedaghatian, N., Barajas, J. F., Wehrs, M., Bailey, C. B.,
615 Kaplan, N., Hillson, N. J., Mukhopadhyay, A., Keasling, J. D. Isolation and
616 characterization of novel mutations in the pSC101 origin that increase copy
617 number. *Sci Rep. 8* (1) (2018), 1590.
618 [49] Averesch, N. J. H., Winter, G., Krömer, J. O. Production of para-aminobenzoic
619 acid from different carbon-sources in engineered Saccharomyces cerevisiae.
620 *Microb Cell Fact. 15* (2016), 89.
621 [50] Koma, D., Yamanaka, H., Moriyoshi, K., Sakai, K., Masuda, T., Sato, Y., Toida,
622 K., Ohmoto, T. Production of p-aminobenzoic acid by metabolically engineered
623 Escherichia coli. *Biosci Biotechnol Biochem. 78* (2) (2014), 350–357.
624 [51] Winkler, R., Richter, M. E. A., Knüpfer, U., Merten, D., Hertweck, C. Regio- and
625 chemoselective enzymatic N-oxygenation in vivo, in vitro, and in flow. *Angew*
626 *Chem Int Ed Engl. 45* (47) (2006), 8016–8018.
627 [52] Lee, J., Simurdiak, M., Zhao, H. Reconstitution and characterization of
628 aminopyrrolnitrin oxygenase, a rieske N-oxygenase that catalyzes unusual
629 arylamine oxidation. *J Biol Chem. 280* (44) (2005), 36719–36728.